Arabian Journal of Chemistry (2015) 8, 518–526

King Saud University

Arabian Journal of Chemistry

www.ksu.edu.sa
www.sciencedirect.com

ORIGINAL ARTICLE

Effect of carbon microfiber materials on sensitivity of adenosine and hydroxyadenine at carbon microfiber sensors

K.M.M. Abou El-Nour *

Department of Chemistry, University of Florida, Gainesville, FL 32611-7200, USA

Received 20 July 2013; accepted 29 August 2013
Available online 7 September 2013

KEYWORDS

Carbon microfiber electrode;
Nanostructured ultramicroelectrode;
Adenosine;
2,8-Dihydroxyadenine;
Carbon fiber sensor;
Fast scan voltammetry

Abstract The relationship between the sensitivity measurements and microfiber electrodes made from different carbon microfiber materials, such as polyacrylonitrile (PAN T650 and PAN HCB) and Pitch P25 was established in this work. The different microfiber electrodes were nanostructured by an electrochemical pretreatment method. Sensitivity of adenosine (ADO) and 2,8-dihydroxyadenine (2,8-DHA) was measured at different carbon microfiber sensors made from different carbon microfiber materials. Sensitivity of PAN microfiber electrodes for ADO and 2,8-DHA determinations measured at 500 V s^{-1} vs. SCE is higher than that measured at Pitch P25 microfiber electrodes due to more defects in PAN microfiber electrodes. Adsorption of ADO and 2,8-DHA is greater at PAN HCB electrodes. High conductivity of PAN fibers correlates with sensitivity determinations of the investigated analytes.

1. Introduction

Microelectrodes exhibit several attractive possibilities, including the exploration of microscopic domains, detection in microflow systems, time-resolved probing of processes in single cells, the *in vivo* monitoring of biological events and analyses of very small sample volumes (Kennedy et al., 1993).

Electrodes of different materials have been miniaturized in many geometrical shapes, with the common characteristic that the electrode dimension is significantly smaller than the diffusion layer at their surface. Due to the greatly reduced double-layer capacitance of microelectrodes, associated with their small area, and radial diffusion to the edges of microelectrodes, the signal-to background characteristics are much better than with conventional electrodes. Because of their geometries and low current intensities, it is possible to work in highly resistive situations, including low dielectric solvents, at low temperatures, in the gas phase, with ionically conductive polymers, and with solutions without the addition of a supporting electrolyte (Stradiotto et al., 2003).

* Permanent address: Department of Chemistry, University of Suez Canal, Ismailia 41522, Egypt. Tel.: +20 643208760; fax: +20 643230416.
E-mail address: kabolnoor@yahoo.com.

Peer review under responsibility of King Saud University.

ELSEVIER Production and hosting by Elsevier

1878-5352 © 2013 Production and hosting by Elsevier B.V. on behalf of King Saud University.
http://dx.doi.org/10.1016/j.arabjc.2013.08.025

For amperometry, a wide range of electrode materials are currently available, including noble metals, boron-doped diamond and a broad spectrum of carbon-based working electrodes. Among carbon-based materials, cylindrical carbon fiber microelectrodes (CFMEs) are widespread tools for monitoring biological events *in vivo* using amperometry and/or voltammetry (Huffman and Venton, 2009). They have also been applied to trace and ultratrace determination of both organic and inorganic electroactive species (Malinski and Taha, 1992; Guzmán et al., 2002).

Carbon fibers are materials made by pyrolysis of suitable precursors with polyacrylonitrile (PAN), pitch, and rayon being the most important. The common feature of the carbon fibers prepared in such a way is their composition from graphitic sheets which can be packed in the following three configurations: (i) radiating out from the center of the fiber (radial type), (ii) aligned in concentric arrangement (onion type), and (iii) distributed randomly (random type) throughout the fiber. The basal plane forms the backbone of the graphitic lattice, and the edge plane contains a significant population of oxygen-containing functional groups. Importantly, the final orientation of the graphitic structure largely determines the electrochemical performance. Because the edge plane of the graphitic sheet is more reactive than the basal plane, the application of a given carbon fiber electrode is dictated by its microstructure.

The sensitivity of carbon fiber electrode (CFE) can be substantially increased by suitable modifications of carbon fiber surface, which include electrochemical conditioning. The electrochemical conditioning (pretreatment) is the preferred carbon fiber modification method due to its good reproducibility, high efficiency, and speed. The essence of the pretreatment is electrooxidation/electroreduction of the fiber's surface, yielding increased amount of surficial oxygen containing functional groups (carbonyl, carboxyl, quinone, ether, ester, and hydroxyl), often denoted as carbon or graphitic oxide (Kepley and Bard, 1988). XPS and Raman studies (Proctor and Sherwood, 1983; Ray and McCreery, 1997) have shown that carbonyl and hydroxyl groups are the predominated surface oxide functionalities on carbon. These moieties can modulate electron transfer rates for many electroactive species and can be specifically blocked using special derivatives (Roberts et al., 2010). This way, the electrode surface properties can be adjusted for an optimum sensitivity toward the desired group of analytes. Besides specific modification of carbon fiber surface by the formation of surficial oxygen-containing groups, nonspecific effects also occur, such as physical removal (etching) of the outer part of carbon fiber, resulting in fiber thinning. Accompanying the process is the increase in electrochemical surface area, typically about five-fold (Kovach et al., 1986), which is also beneficial for higher current densities achieved on "pretreated" fibers.

Analytical response of carbon fiber electrodes has been related to tensile modulus of the fibers (De Carvalho et al., 2001). A direct relationship between carbon fiber tensile modulus and electrical conductivity has been reported (Minus and Kumar, 2005), but not with the precursor material of the fiber (Huffman and Venton, 2008). However, the method of carbon fiber electrode surface fabrication may have contributed to the observed behaviors (Huffman and Venton, 2008). Since electrochemistry is based fundamentally on interfacial phenomena, the structure and chemistry of the electrode surface are of obvious importance (McCreery, 2008).

Adenosine is a purine nucleotide that performs many important functions in the human body and biological processes (Cummings et al., 1994). It modulates physiological functions in the heart and brain, regulates oxygen supply during cell stress and plays an important role in the regulation of renal functions (Zhang et al., 1997; Kloor et al., 2000).

Adenine is one of the purine nucleobases and is therefore an essential molecule of life and evolution. Adenine is a component of adenosine, according to the previous studies of adenine oxidation it was concluded that the first $2e^-$, $2H^+$ oxidation of adenine leads to 2-hydroxyadenine which on further $2e^-$, $2H^+$ oxidations form 2,8 dihydroxyadenine as is reported for adenine in the literature (Kathiwala et al., 2010; Goyal and Sangal, 2002).

In this work, a direct measurement of the effect of material structure on electrochemical performance of carbon fiber microdisk electrodes was done. The electrodes were made by a method, which produces stable and renewable electrodes (Brajter-Toth et al., 2000; Kathiwala et al., 2008, 2010); stability of the electrodes is due to the limited overoxidation of the electrode surface. The surface nanostructures of the electrodes have been characterized (Brajter-Toth et al., 2000; Kathiwala et al., 2008). Fast scan measurements were successfully done at such electrodes. In addition, fast scan methods facilitate the acquisition of a large number of signals that can be averaged in a short period of time, and allow for kinetic filtering, which reduces interference effects (Bravo et al., 1998).

Both adenosine (ADO) and 2,8-dihydroxyadenine (2,8-DHA) adsorb weakly at carbon fiber electrodes and undergo fast electron transfer kinetics (Abou El-Nour and Brajter-Toth, 2000; Kathiwala et al., 2010), they produce highly reproducible signals at carbon fiber electrodes These characteristics make them suitable as electrochemical probes for characterizing the nanostructured surfaces by FSV at 500 V s^{-1}. The results confirm contributions of material properties to electroanalytical performance of carbon fiber electrodes. The observed correlations between material properties and electrochemical parameters are discussed.

2. Experimental

2.1. Reagents and methods

All chemicals were of the analytical reagent grade and were used as received. 6-amino-1H-purine-2,8-dione i.e., (2,8-dihydroxyadenine) and adenosine were obtained from Sigma-Aldrich, St. Louis, MO. All other chemicals were obtained from Fisher Scientific (Pittsburgh, PA). Solutions were prepared in doubly deionized water daily before experiments. Phosphate buffer, pH 7.4, contained sodium phosphate monobasic monohydrate ($NaH_2PO_4.H_2O$) and dibasic anhydrous (Na_2HPO_4) at a total concentration of 31 mM was used. The pH of solutions was adjusted with NaOH or HCl before experiments.

Adenosine (ADO) and 2,8-dihydroxyadenine (2,8-DHA) were prepared before the experiments in 31 mM phosphate buffer (pH 7.4). Potassium ferricyanide was prepared in 0.5 M KCl (pH 6.0). All determinations were performed at room temperature. The percentage of CO_2 in air of 0.03%

and of oxygen of 21% was not changed and the solutions were not purged with gases. The sensitivity of each analyte was determined from the slopes of the calibration curves. At least 8 points for each calibration curve and 4 determinations at each concentration were obtained at three different electrodes. The results obtained at different CFEs were pooled. All other measurements were repeated at least in triplicate. The reported results reflect the reproducibility of the measurements and the reproducibility of fabrication of carbon fiber sensors.

2.2. Instrumentation

The instrumental set up has been described previously (Kathiwala et al., 2010). Bioanalytical Systems Electrochemical Analyzer (BAS-100, West Lafayette, IN) with a home-built preamplifier was interfaced to a PC and was used in slow scan cyclic voltammetry. A two-electrode configuration was used, with CFE as working and SCE as reference. In slow scan voltammetry, the potential scan rate was (50 mV s^{-1}); the potential window was −0.2 to 0.5 V for ferricyanide.

Fast-scan cyclic voltammetry (FSV) was performed with signal averaging and with digital background subtraction (Brajter-Toth et al., 2000). Briefly, a triangular waveform was applied with a function generator (Universal Programmer, Model 175, EG&G Princeton Applied Research, Princeton, NJ, USA) to a SCE in a two electrode configuration. Current at CFE was converted into voltage and amplified by a home-built current-to-voltage converter and was recorded and stored by a digital oscilloscope (LeCroy Model 9310, Chestnut Ridge, NY, USA). A copper mesh Faraday cage was used to minimize noise.

The solutions were injected into ca. 80 μL electrochemical cell with a syringe and a permanent electrode-solution contact was maintained. In FSV, the background current was recorded in buffer first, before each analytical signal was recorded, and was signal averaged and stored by the digital oscilloscope. The analytical signal was obtained immediately afterward, and was signal averaged and stored by the digital oscilloscope in a separate channel. The stored background current was subtracted from the stored analytical signal using the digital oscilloscope. The background subtracted analytical signal was transferred from the digital oscilloscope to a personal computer. ADO and 2,8-DHA signals were recorded in the same potential window as the background current from −1.0 to 1.5 V, under the same experimental conditions. Number of cycles in FSV was 250 (Hsueh and Brajter-Toth, 1996). In FSV the potential scan rate was 500 Vs^{-1}. Data obtained from FSV were analyzed with Origin (Microcal Software, Inc. Northampton, MA) using a PC.

2.3. Electrodes

A saturated calomel electrode (SCE) was used as a reference electrode and carbon fiber microdisk electrodes (CFMEs) were used as working electrodes. Fabrication of carbon fiber microdisk electrodes has been described (Brajter-Toth et al., 2000; Bravo et al., 1998).

PAN T650 (PAN I), Pitch P25 (PT) (Cytec Engineered Materials, Greenville, SC), and PAN HCB (PAN II) (Textron Specialty Materials, Lowell, MA) fibers were used to fabricate the microdisk working electrodes (carbon assay % is 94, 99.5 and 99+, respectively). The fiber (ca. 3 cm long) was connected to copper wire (ca. 6 cm long, 0.3 mm diameter, Fisher Scientific, Pittsburgh, PA) with electrically conductive silver epoxy (E4110 part A, Epoxy Technology, Billerica, MA) mixed with 40 wt.% of curing agent (hardener) (E4110 Part B).

Approximately 1 cm of the fiber and wire was covered by the epoxy mixture, and the assembly was cured at room temperature for 48 h. The copper wire end of the electrode assembly was drawn into a 200 mL micropipette tip (5 cm long) so that ca. 1 cm of the fiber was drawn in. The pipette tip was filled with a hot (80–90 °C) mixture of epoxy (EPON Resin 828, Miller-Stephenson Chemical Co., Danbury, CT) with 10 wt.% m-phenylenediamine flaked hardener (DuPont Specialty Chemicals, Wilmington, DE). To obtain a good quality seal, the resin was cured for 72 h at room temperature. The sealed electrodes were further cured at 90 °C for 1 h to improve their mechanical properties.

The cross sectional surface of the fiber was exposed by touch-polishing with 600 grit SiC polishing paper (Mark V Laboratory, East Granby, CT), mounted on a polishing wheel (Ecomet I, Buehler Ltd, Evanston, IL) with doubly distilled water as a lubricant.

Electrodes were held at approximately the right angle to the surface of the polishing paper in order to obtain a disk-shaped surface.

Because of the well-known redox properties and limited adsorption (Abou El-Nour and Brajter-Toth, 2000), potassium ferricyanide was used in the determination of the apparent electrode radius, r. The radius was determined from the limiting current of ca. 5 mM $Fe(CN)_6^{3-}$ in 0.5 M KCl by cyclic voltammetry at 50 mV s^{-1}, from 0.5 to −0.2 V, using Eq. (1) for steady-state disk current (Bard and Faulker, 2004).

$$i_{ss} = 4nFD_0C_0^*r \quad (1)$$

where i_{ss} denotes the steady-state limiting current (nA) at −150 mV, n is the number of electrons (which equals 1 in the reduction of $Fe(CN)_6^{3-}$), F is Faraday's constant, C_0^* is the bulk concentration (5 mM) of $Fe(CN)_6^{3-}$ and D_0 is the diffusion coefficient of $Fe(CN)_6^{3-}$ (approximated at 7.6×10^{-6} cm^2 s^{-1} from (Bard and Faulker, 2004) under similar conditions).

The limiting current of ferricyanide was additionally measured to verify the reproducibility of fabrication of carbon fiber microdisk electrodes from log-plot analysis of the i–E curves of ferricyanide and from the value of $E^{0'}$ determined from $E^{1/2}$ (Abou El-Nour and Brajter-Toth, 2000).

Nanostructured microdisk electrode surfaces were obtained by an electrochemical pretreatment (ECP) method, as previously described (Kathiwala et al., 2010).

Briefly, this involves continuous potential cycling from −1.0 to 1.5 V, at 10 V s^{-1} for 30 min in 31 mM phosphate buffer, pH 7.4. Electrodes that produced fast kinetics of $Fe(CN)_6^{3-}$, determined from the analysis of E vs. $\log[(i_L - i)/i]$ plots (Abou El-Nour and Brajter-Toth, 2000) and well-developed steady-state voltammograms were used for FSV measurements of ADO and 2,8-DHA at 500 V s^{-1}. Electrodes, which had excessively noisy background current at 500 Vs^{-1} and produced irreproducible background subtracted signals, were discarded.

The CFE quality was additionally confirmed from the measurement of the electrode capacitance (Bravo and Brajter-Toth, 1999; Brajter-Toth et al., 2000).

Apparent specific electrode capacitance, C (μF cm^{-2}), was determined before and after ECP, and after FSV measurements, from the background current at 0.75 V (Bravo and Brajter-Toth, 1999) in 31 mM phosphate buffer pH 7.4 at 10 V s^{-1}. Eq. (2) was used to calculate the apparent electrode capacitance. It was assumed that the background current at 0.75 V results predominantly from double-layer charging, with limited contributions of surface faradaic reactions (Brajter-Toth et al., 2000).

$$C_{obs} = \Delta i/2\nu A \quad (2)$$

where Δi represents the difference between anodic and cathodic sections of the background current, ν is the potential scan rate at 10 V s^{-1}, A is the geometric area of the microdisk electrode (cm^2) calculated based on the geometric radius of the fiber. The CFE capacitance values that were obtained are summarized in Table 1. The ratio of C_{obs} of the microdisk electrode after ECP to the specific capacitance of the edge plane highly ordered pyrolytic graphite (CHOPG = 60 μF cm^{-2}) (Rice and McCreery, 1989) was calculated to estimate the roughness factor of the nanostructured electrodes.

2.4. Fast scan voltammetry

FSV measurements were performed as described before (Hsueh et al., 1997). The sequential acquisition of background and analyte signal, in the same potential window and at the same potential scan rate, has been optimized to minimize irreversible surface reactions (Brajter-Toth et al., 2000; Kathiwala et al., 2008, 2010). This produces reproducible signals and stable electrodes that can be reused, and allows accurate digital background subtraction (Brajter-Toth et al., 2000; Kathiwala et al., 2008, 2010).

Signal averaging was used and the number of scans recorded was a compromise between high signal-to-noise (S/N) ratio and measurement time (Hsueh et al., 1997). The reported values are averages of measurements for at least four electrodes. Geometric area was used to obtain normalized values of anodic peak current of probes and background current at electrodes.

2.5. Analytical determinations

The sequential acquisition of the background and the analyte currents, in the same potential window and at the same potential scan rate, facilitates accurate digital background subtraction (Brajter-Toth et al., 2000; Hsueh et al., 1997). This procedure was repeated for all calibrations in the measurement ranges. ADO and 2,8-DHA were determined in 31 Mm phosphate buffer, pH 7.4, by FSV at 500 V s^{-1}.

Sensitivity is reported as the average slope of the calibration curve for at least 8 concentrations and 4 determinations at each concentration at three different carbon microfiber electrodes. Data were processed using Origin software (Origin Lab, Northampton, MA).

3. Results and discussion

3.1. Electrochemical measurements of carbon fiber electrodes

3.1.1. Response to ferricyanide

Electrochemical pretreatment (ECP) methods (Takmakov et al., 2010; Brajter-Toth et al., 2000; Kathiwala et al.,

Table 1 Surface properties and sensitivity of microfiber electrodes.

Type of micro-fiber electrodes	r^a(μm)		$E^1/_2$[b](mV)		CFE[c]Capacitance (μF cm^{-2})		i^d(nA)	Roughness factor	Sensitivity[e](nA μM^{-1})	
	Before ECP	After ECP	Before ECP	After ECP	Before ECP	After ECP			ADO	2,8-DHA
PAN I	2.8 ± 0.3	3.0 ± 0.4	175 ± 40	206 ± 5	392	834	4.5	13.9	0.34 ± 0.04	0.40 ± 0.01
PAN II	3.1 ± 0.8	3.3 ± 0.9	140 ± 45	208 ± 5	488	844	4.9	14.1	0.38 ± 0.08	0.45 ± 0..01
PT	4.3 ± 0.4	4.5 ± 0.8	116 ± 44	210 ± 4	577	1444	7.9	24.1	0.24 ± 0.08	0.26 ± 0.03

[a] Apparent radius of electrodes from slow scan voltammetry of 5 mM $K_3Fe(CN)_6$, 0.5 M KCl; 50 mV s^{-1}, Eq. (1).
[b] From Fig. 1.
[c] From background current at 0.75 V, 31 mM phosphate buffer, pH 7.4, scan rate 10 V s^{-1}, 50 cycles averaged, potential window −1.0 to 1.5 V, Eq. (2) and Fig. 2.
[d] Background current at 1.0 V, from cyclic voltammetry, scan rate 10 V s^{-1}, 50 cycles averaged.
[e] From linear part of calibration curves of adenosine and 2,8-dihydroxyadenine in 31 mM phosphate buffer, pH 7.4 at 500 V s^{-1}, 250 cycles averaged. Potential window: −1.0 to 1.5 V. At least eight concentrations for each calibration curve, four determinations at each concentration, at three different CFEs.

2008, 2010) are used for etching the carbon fiber electrode surface and consequently forming surface nanocracks and edge nanostructures. These methods can lead to irreversible side reactions such as electrolysis of water, production of carbon dioxide and the formation of non-conducting surface oxides. These reactions can contribute to irreversible behavior of carbon fiber electrodes (Brajter-Toth et al, 2000; Kathiwala et al., 2008, 2010; Goss et al., 1993). However, solution composition, potential window, potential scan rate and waveform, used during surface nanostructured formation by ECP, can be optimized to control these reactions (Brajter-Toth et al, 2000; Bravo et al., 1998).

Electron transfer kinetics of ferricyanide are determined by electrode surface structure and are used to detect electrode activity (McCreery, 2008; Brajter-Toth et al, 2000). Fig. 1 shows cyclic voltammograms of 5 mM $Fe(CN)_6^{3-}$ at PAN I, PAN II and PT carbon microfiber electrodes in 0.5 M KCl. Slow electron transfer kinetics of ferricyanide are typically observed at polished and non-treated carbon fiber electrodes (Fig. 1, solid line), in spite of carbon fiber material. This is apparent from the slow rise in ferricyanide current and the poorly-defined limiting current plateau of ferricyanide (Fig. 1, solid line). On contrary ferricyanide kinetics are fast at electrodes modified by ECP (Fig. 1, small dash). This is apparent from higher $E_{1/2}$ values and well-defined plateaus of the i–E curves (Fig. 1, small dash). As mentioned before (Brajter-Toth et al, 2000; Kathiwala et al., 2008, 2010) nanostructured carbon microfiber electrodes formed by electrochemical nanostructured of the surface by ECP have a stable background current and the electrode surface can be easily renewed by FSV.

However, after the ECP of the electrode surface, differences in response to ferricyanide are observed at the nanostructured microdisk electrodes made from different carbon fiber materials.

After ECP as shown in Fig. 1 (small dash), at PAN I carbon fiber electrodes, the limiting current of ferricyanide decreases while it increases at PAN II and PT carbon microfiber electrodes.

These differences can be attributed to the carbon fiber material properties since the fabrication conditions of electrode surface are the same. Electrodes from the two types of PAN fibers (I and II) have a similar geometric radius (Table 1). However, carbon assay fibers are relatively low 94% for PAN I while it equals 99.5% in case of PAN II fibers, also the electrical conductivity of PAN I is lower than that of PAN II (667 and 909 S cm^{-1}, respectively) (Laffont et al., 2004).

The conductivity, material disorder and crystalline structure of PAN-based carbon microfibers have been confirmed by different methods of analysis (Kim et al., 2004). From these analyses it was found that lower carbon assay indicates more amorphous structure of PAN I fibers. Less ordered fiber structure facilitates oxidation (Pamula and Rouxhet, 2003) of PAN I carbon fiber electrode surfaces during surface nanostructured formation by ECP.

Great ability of less crystalline carbon fibers to oxidation has been verified by X-ray photoelectron spectroscopy (Pamula and Rouxhet, 2003) and hence greater surface oxide coverage is expected. Ferricyanide access to oxide rich surfaces can be repressed (Cheng and Brajter-Toth, 1996) as observed here. Consequently, PAN I, PAN II and PT carbon microfiber electrodes, although fabricated by the same method, will have different surface structures and chemistry, which results from different properties of the respective carbon fiber materials.

The electron transfer kinetics of ferricyanide at polished and non-treated PAN I carbon fiber electrodes are faster than at electrodes made from PAN II and PT carbon fibers, as indicated by more positive $E_{1/2}$ values (Table 1) and lower slope of E vs. $\log[(i_L - i)/i]$ plots for ferricyanide at these microelectrodes. Faster kinetics at polished and non-treated PAN I electrodes are consistent with greater material disorder of PAN I carbon fiber material (Cheng and Brajter-Toth, 1996). Kinetics of ferricyanide is even faster at these electrodes after the surface is nanostructured by ECP. This is verified by the positive shift in $E_{1/2}$ and the lower slope values of log-plots that were obtained from the slow scan voltammetry $i - E$ curves of ferricyanide which had slope close to 59 ± 0.1 mV at all electrodes, that were made from different carbon fiber materials which is expected for a one-electron reversible reaction (Bard and Faulker, 2004). After ECP, $E_{1/2}$ values are close to $E^{0'}$ of 210 mV (vs. SCE) which has been reported for $Fe(CN)_6^{3-/4-}$ in 0.5 M KCl (Bard, 1928). Thus, electrode kinetics of ferricyanide, after ECP of the electrodes, is independent of the electrode carbon fiber material (Whitson et al., 1973).

3.1.2. Background current and electrode capacitance

It was reported before that high electrode background current reflects high electrode surface area of nanostructured carbon fiber electrodes (Brajter-Toth et al., 2000; Kathiwala et al., 2008, 2010). Fig. 2 confirms this at electrodes made from different carbon fiber materials. It is observed from Fig. 2 that the lowest background current is shown at PAN I electrodes, which is due to their small geometric radius. The specific capacitance calculated from the normalized background currents using Eq. (2) is similar at electrodes fabricated from

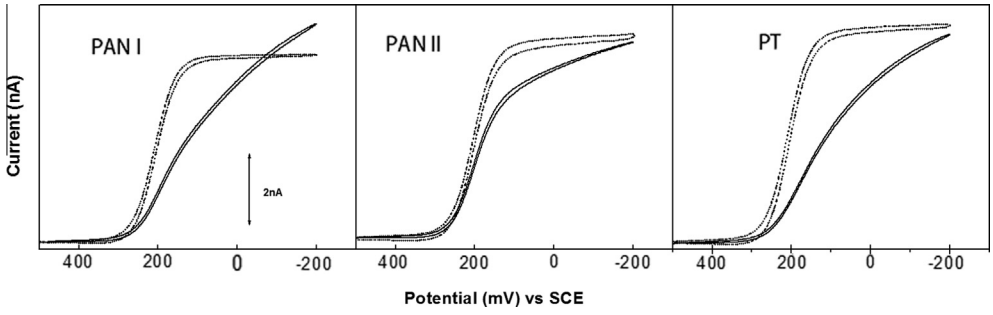

Figure 1 Cyclic voltammetry of different microfiber electrodes in 5 mM $K_3Fe(CN)_6$, 0.5 M KCl, 50 mV s^{-1}, 31 mM phosphate buffer pH 7.4, before (solid line) and after (dotted line) electro-chemical pretreatment of electrode surface.

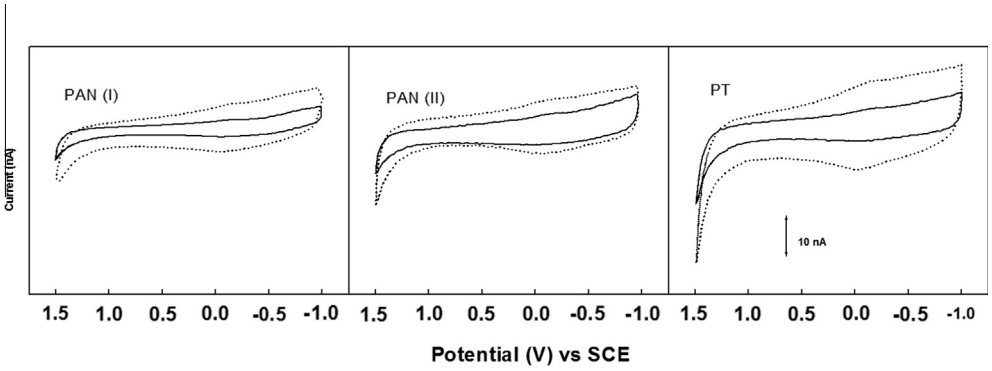

Figure 2 Voltammetric background current at different carbon microfiber electrodes before (solid line) and after (dotted line) electrochemical pretreatment at pH 7.4 in 31 mM phosphate. Scan rate 10 V s^{-1}, 50 cycles averaged.

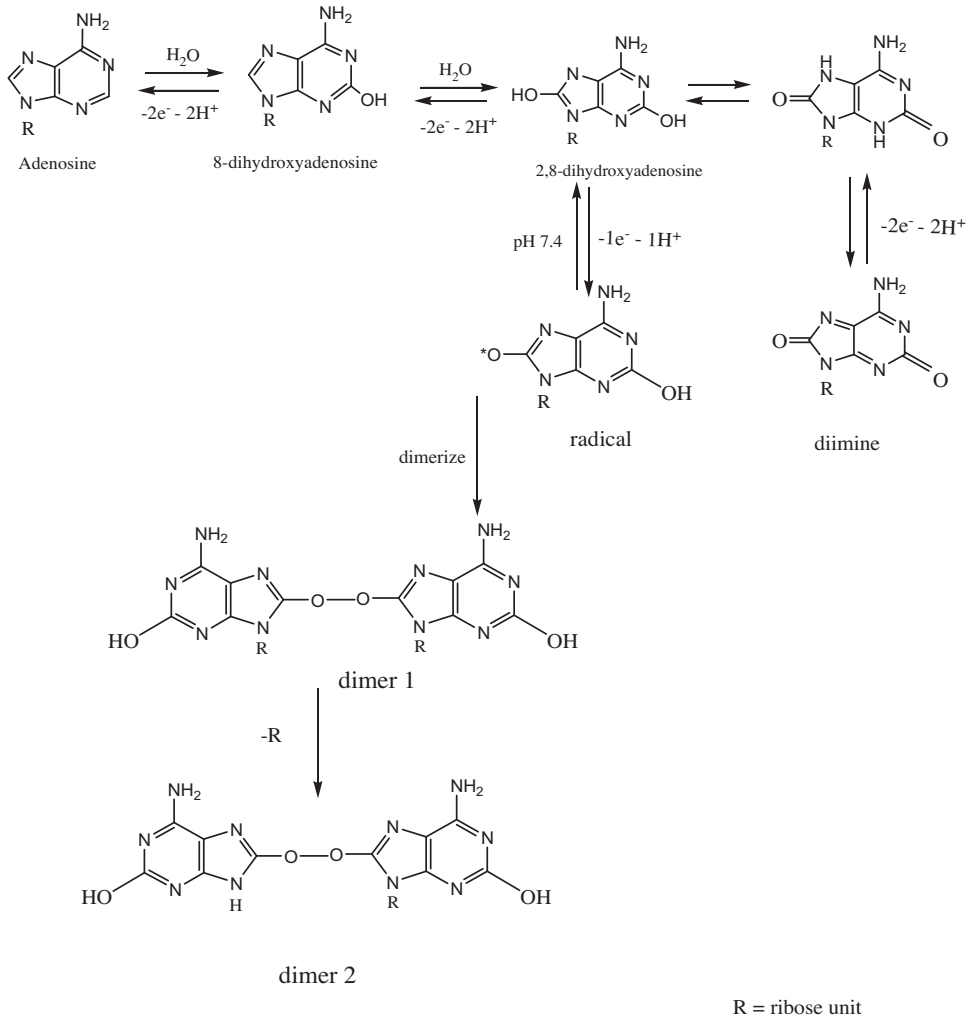

Scheme 1 Reaction mechanism proposed for the electrooxidation of adenosine Goyal et al. (1991)

PAN I and PAN II materials and is higher at PT electrodes, which have a larger geometric radius. (Table 1).

Electrodes from the two types of PAN fibers have similar surface roughness factors due to their similar (apparent) specific capacitance (Table 1), although carbon content and electrical conductivity of PAN II fibers are higher than those of PAN I fibers.

The differences in surface roughness reflect the differences in the properties of different carbon fiber materials such as carbon assay, surface area, and density.

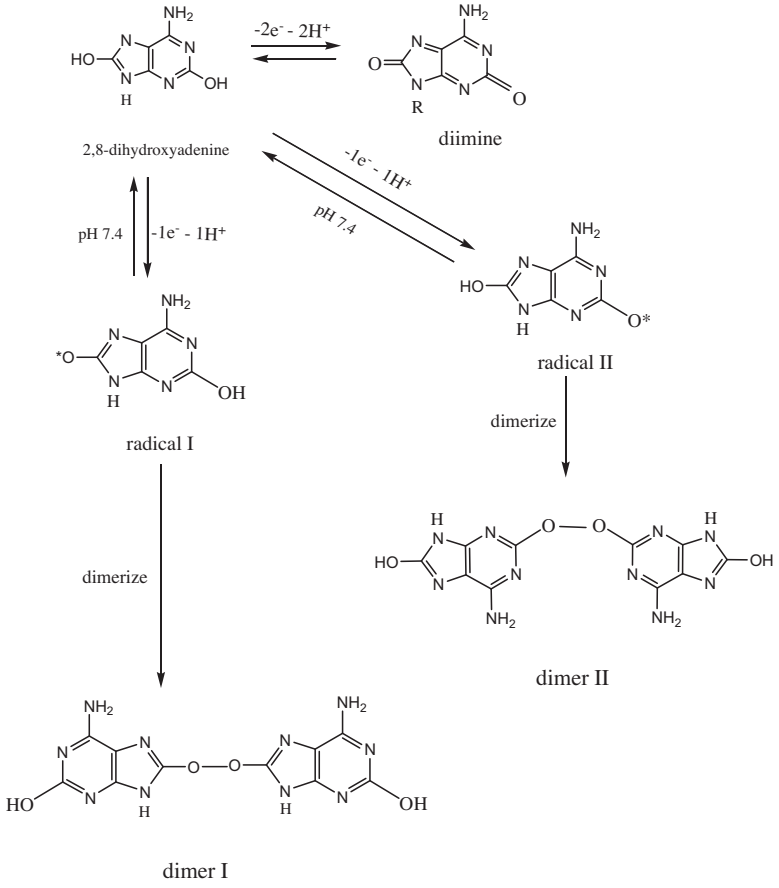

Scheme 2 Proposed electrochemical oxidation pathway of 2,8-dihydroxyadenine Kathiwala et al. (2010).

3.2. Electrode reaction of ADO and 2,8-DHA

The oxidation of adenosine proceeds in a mechanism involving a $6e^-$, $6H^+$ process to give 2-hydroxyadenosine and 2,8-dihydroxyadenosine and then the corresponding diimine Scheme 1. .

Also, 2,8-dihydroxyadenine is oxidized in a $2e^-$, $2H^+$ step to give the corresponding diimine Scheme 2.

Formation of the diimine and its short half-life (~50 ms) in case of various purines at different electrodes has already been documented in the literature (Wopshall and Shain, 1967; Brown and Large, 1964). The oxidation potentials of hydroxypurines have been found to be less positive in comparison with simple purines (Lingane, 1966).

It appears that 2,8 dihydroxyadenosine and 2,8-DHA undergo $1e^-$, $1H^+$ oxidation to give a radical species which rapidly dimerizes with another similar moiety to form dimer as is shown in Schemes 1–2. Oxidation of 8-hydroxypurines in a $1e^-$, $1H^+$ step to form a variety of dimers has been documented in the literature (Furniss et al., 1994; Swern, 1971).

Also, for adenosine it was reported before (Goyal et al., 1991) that one of the ribose units of the initial O–O dimer is removed due to steric hindrance in the dimer during its formation. Hence, one of the ribose units is hydrolyzed to give another dimer (Scheme 1).

As shown in Fig. 3, oxidation of 10 μM ADO results in a well-developed oxidation peak observed at ca. 0.98 V and a

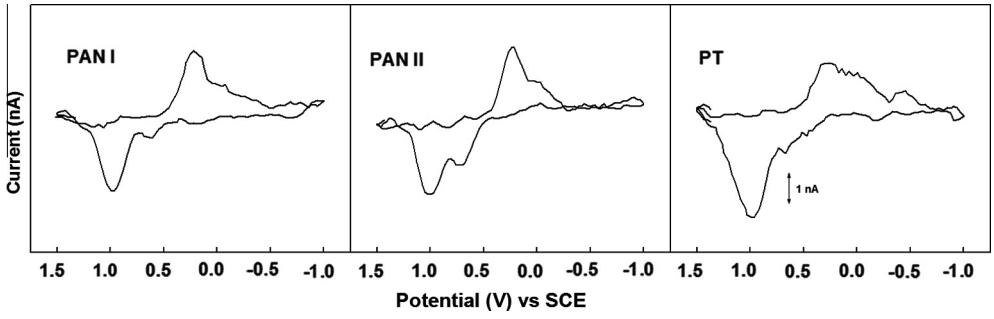

Figure 3 Fast scan cyclic voltammograms of 10 μM Adenosine at different carbon microfiber electrodes, in 31 mM phosphate buffer pH 7.4, 500 V s^{-1}, 250 cycles, results after background subtraction.

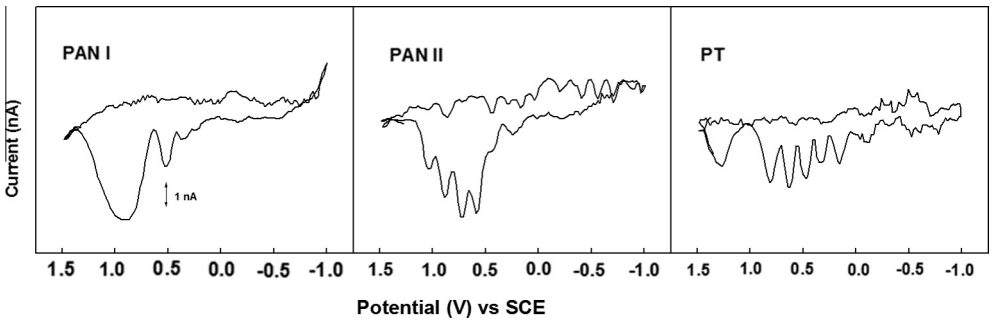

Figure 4 Fast scan cyclic voltammograms of 10 μM 2,8-dihydroxyadenine at different carbon microfiber electrodes, in 31 mM phosphate buffer, pH 7.4, 500 V s^{-1}, 250 cycles, results after background subtraction.

shoulder at ca. 0.65 V in the case of PAN I microfiber electrode. The observed peaks shifted to more positive potentials at ca.1.0 V and 0.7 V, respectively in the case of PAN II microfiber electrode, while the oxidation of ADO at a PT microfiber electrode results in one broad large peak at ca. 0.97 V and a shoulder at 0.68 V.

On the other hand, from Fig. 4, oxidation of 10 μM 2,8-DHA produces one broad large peak at ca. 0.90 V, small peak at 0.52 V and a shoulder at 0.35 V at PAN I microfiber electrode. Multiple small peaks were observed in the case of PAN II and PT microfiber electrodes. At PAN II small peaks were observed at ca. 1.0, 0.87, 0.71, 0.57 and 0.23 V, respectively as well as a shoulder at 0.41 V. In PT microfiber electrode the multiple small peaks shifted to less positive potentials and appeared well-developed at ca. 0.8, 0.63, 0.47, 0.32, 0.15 V, respectively.

Peaks observed at ca. 0.98 V in ADO voltammograms and at ca. 0.8 V were measured to obtain ADO and 2,8-DHA calibration curves, respectively (Abou El-Nour and Brajter-Toth, 2000; Kathiwala et al., 2010).

Current traces between 0 and 0.1 V and ca. 1.2 V (Figs. 3 and 4) are likely due to products resulting from the incomplete background subtraction.

Reduction of diimine is likely responsible for the reduction peaks between ca. −0.27 V and −0.36 V Figs. 3 and 4. The reduction of diimine followed by reoxidation process is quite fast as shown by the near reversibility of the oxidation/reduction peaks in the voltammograms of ADO and 2,8-DHA.

Large surface area of nanostructured carbon fiber electrodes favors adsorption. Peak potentials for the forward and reverse processes are close, suggesting adsorption of both ADO and 2,8-DHA. The proton-coupled electron transfer of ADO and 2,8-DHA at pH 7.4 can aid interactions with surface oxides. High analytical sensitivity of ADO and 2,8-DHA reflects high adsorption behavior at carbon microfiber electrodes which consecutively reveals structure of the electrode surfaces (Maldonado et al., 2006; O'Mullane et al., 2008). High anodic peak currents of ADO and 2,8-DHA at 500 V s^{-1} indicate adsorption-controlled processes.

The relative magnitudes of the peak currents for ADO at different electrodes are PAN I ≈ PAN II > PT indicating more adsorption at PAN electrodes (Fig. 3). 2,8-DHA adsorbs more than ADO at PAN I electrodes as the magnitudes of the peak currents at different microfiber electrodes are in the order PAN I > PAN II > PT (Fig. 4). The results show that 2,8-DHA adsorbs highly at more disordered PAN I than at PAN II and PT electrodes.

Adsorption of 2,8-DHA at PAN electrodes is higher than that of ADO at the same electrodes this may be related to the steric hindrance due to the existence of ribose unit in the ADO structure.

3.3. Electrode sensitivity

Low adsorption and sensitivity of ADO and 2,8-DHA at pitch microfiber electrodes (Figs. 3 and 4 and Table 1), are expected as a result of small change in electrode surface results from ECP of these microfiber electrodes (Table 1). Although the two types of PAN electrodes have similar surface areas after ECP, PAN II electrodes are significantly more sensitive in ADO and 2,8-DHA measurements. This may be due to high material disorder (defects) of the surface of PAN I which facilitates over oxidation of the electrode surface, generating greater surface oxide coverage and subsequently less adsorption of ADO and 2,8-DHA.

The higher sensitivity of PAN II electrodes matches lower defects and higher electrical conductivity of PAN II fibers (909 S cm^{-1}) than PAN I (667 S cm^{-1}).

Slower kinetics at PAN I than at PAN II electrodes reflect higher material defect and expected higher degree of surface oxidation of PAN I.

Methods of carbon fiber electrode surface treatment/reactivation used here, which likely produce defects and cation-exchanged surface oxides, ultimately lead to high sensitivity in ADO and 2,8-DHA determinations by fast-scan voltammetry (Table 1).

ADO and 2,8-DHA have faster kinetics at more ordered, and presumably less oxidized PAN II carbon fiber electrodes which correlate with more adsorption and greater sensitivity. Thus, structure and composition of carbon fiber materials influence surface interactions of the microfiber electrode.

4. Conclusions

Less oxidized and less disordered PAN II electrodes show more adsorption of ADO and 2,8-DHA. Also PAN microfiber electrodes have smaller geometric radius than pitch microfiber electrodes, this leads to lower the background current and thus give better signal subtraction which increased sensitivity of ADO and 2,8-DHA measurements.

In addition, greater geometric radius of pitch microfiber electrodes reduces the formation of nanofeatures and surface oxides at the electrode surface during the surface nanostructure formation by electrochemical pretreatment.

Thus, the behavior of nanostructured carbon microfiber electrodes prepared by the same method of ECP depends on the structure of carbon fiber materials. The results that were obtained in this work afford the correlation between carbon microfiber electrode materials and electrode properties such as activity and sensitivity.

Acknowledgments

This work was personally funded at Department of Chemistry, University of Florida, Gainesville, Florida, USA. I would like to sincerely thank Prof. Anna Brajter-Toth for her cooperation in using her research laboratory at the Department of Chemistry, University of Florida to do this work, and also for her helpful discussion. I would also like to thank Dr. Mehjabin Kathiwala and Dr. Abraham Boateng from University of Florida for their help in laboratory work.

References

Abou El-Nour, K., Brajter-Toth, A., 2000. Electroanalysis 12, 805.
Bard, A.J., 1928. Encyclopedia of Electrochemistry of the Elements. Marcel Dekker, New York, part A, 9, 236.
Bard, A.J., Faulker, L.R., 2004. Electrochemical Methods, 2nd ed. Wiley, New York.
Brajter-Toth, A., Abou El-Nour, K., Cavalheiro, E.T., Bravo, R., 2000. Anal. Chem. 72, 1576.
Bravo, R., Brajter-Toth, A., 1999. Chem. Anal. (Warsaw) 44, 423.
Bravo, R., Hsueh, C.C., Brajter-Toth, A., Jaramillo, A., 1998. Analyst 123, 1625.
Brown, E.R., Large, R.F., 1964. Physical Methods of Chemistry. Wiley Interscience, Rochester, New York.
Cheng, Q., Brajter-Toth, A., 1996. Anal. Chem. 68, 4180.
Cummings, J., Leonard, R.C.F., Miller, W.R., 1994. J. Chromatogr. B 658, 183.
De Carvalho, R.M., De Oliveira Neto, G., Kubota, L.T., 2001. Electroanalysis 13, 131.
Furniss, B.S., Hannaford, A.J., Smith, P.W.G., Tatchell, A.R., 1994. Vogel's, Textbook of Practical Organic Chemistry. ELBS with Longman, UK.
Goss, C.A., Brumfield, J.C., Irene, E.A., Murray, R.W., 1993. Anal. Chem. 65, 1378.
Goyal, R.N., Sangal, A., 2002. J. Electroanal. Chem. 521, 72.
Goyal, R.N., Kumar, A., Mittal, A., 1991. J. Chem. Soc., Perkin Trans. 2, 1369.
Guzmán, A., AğúI, L., Pedrero, M., Ýa~nez-Sede~no, P., Pingarŕ, J.M., 2002. Talanta 56 (3), 577.
Hsueh, C.C., Brajter-Toth, A., 1996. Anal. Chim. Acta 321, 209.
Hsueh, C.C., Bravo, R., Jaramillo, A.J., Brajter-Toth, A., 1997. Anal. Chim. Acta 349, 67.
Huffman, M.L., Venton, B.J., 2008. Electroanalysis 20, 2422.
Huffman, M.L., Venton, B.J., 2009. Analyst 134 (1), 18.
Kathiwala, M., Affum, A.O., Perry, J., Brajter-Toth, A., 2008. Analyst 133, 810.
Kathiwala, M., El-Nour, K.A., Cohen-Shohet, R., Brajter-Toth, A., 2010. Analyst 135, 296.
Kennedy, R., Huang, L., Atkinson, M., Dush, P., 1993. Anal. Chem. 65, 1882.
Kepley, L.J., Bard, A.J., 1988. Anal. Chem. 60 (14), 1459.
Kim, C., Park, S.H., Cho, J.I., Lee, D.Y., Park, T.J., Lee, W.J., Yang, K.S., 2004. J. Raman Spectrosc. 35, 928.
Kloor, D., Yao, K., Delabar, U., Osswald, H., 2000. Clin Chem 46, 537.
Kovach, P.M., Deakin, M.R., Wightman, R.M., 1986. J. Phys. Chem. 90 (19), 4612.
Laffont, L., Monthioux, M., Serin, V., Mathur, R.B., Guimon, C., Guimon, M.F., 2004. Carbon 42, 2485.
Lingane, J.J., 1966. Electroanalytical Chemistry. Wiley, New York.
Maldonado, S., Morin, S., Stevenson, K.J., 2006. Analyst 131, 262.
Malinski, T., Taha, Z., 1992. Nature 358 (6388), 676.
McCreery, R.L., 2008. Chem. Rev. 108, 2646.
Minus, M.L., Kumar, S., 2005. JOM 57, 52.
O'Mullane, A.P., Zhang, J., Brajter-Toth, A., Bond, A.M., 2008. Anal. Chem. 80, 4614.
Pamula, E., Rouxhet, P.G., 2003. Carbon 41, 1905.
Proctor, A., Sherwood, P.M.A., 1983. Carbon 21 (1), 53.
Ray, K., McCreery, R.L., 1997. Anal. Chem. 69 (22), 4680.
Rice, R.J., McCreery, R.L., 1989. Anal. Chem. 61, 1637.
Roberts, J.G., Moody, B.P., McCarty, G.S., Sombers, L.A., 2010. Langmuir 26 (11), 9116.
Stradiotto, N.R., Yamanaka, H., Zanoni, M.V.B., 2003. J. Braz. Chem. Soc. 14 (2), 159.
Swern, D., 1971. Organic Peroxides. Wiley Interscience, New York.
Takmakov, P., Zachek, M.K., Keithley, R.B., Walsh, P.L., Donley, C., McCarty, G.S., Wightman, R.M., 2010. Anal. Chem. 82, 2020.
Whitson, P.E., Born, H.W.V., Evans, D.H., 1973. Anal. Chem. 45, 1298.
Wopshall, R.H., Shain, I., 1967. Anal. Chem. 39, 1514.
Zhang, J.H., Belardinelli, L., Jacobson, K.A., Otero, D.H., Baker, S.P., 1997. Mol. Pharmacol. 52, 491.